QUADRATURE VCO FORMED WITH TWO COLPITTS VCO COUPLED VIA AN LC-RING RESONATOR

S.-L. Jang, S.-S. Lin, C.-W. Chang[*], and S.-H. Hsu

Department of Electronic Engineering, National Taiwan University of Science and Technology, 43, Keelung Road, Section 4, Taipei, Taiwan 106, Republic of China

Abstract—This paper presents a new quadrature voltage-controlled oscillator (QVCO), which consists of two p-core Colpitts cross-coupled voltage-controlled oscillators (VCOs) with an LC ring resonator to provide the quadrature outputs. The proposed CMOS QVCO has been implemented with the TSMC 0.18 μm CMOS technology and the die area is $0.478 \times 0.82 \, \text{mm}^2$. At the supply voltage of 1.5 V, the total power consumption is 20.4 mW. The free-running frequency of the QVCO is tunable from 9.69 GHz to 10.52 GHz as the tuning voltage is varied from 0.0 V to 2 V. The measured phase noise at 1 MHz frequency offset is -122.41 dBc/Hz at the oscillation frequency of 10.52 GHz and the figure of merit (FOM) of the proposed QVCO is -189.7 dBc/Hz.

1. INTRODUCTION

CMOS quadrature voltage controlled oscillators (QVCOs) are essential circuit blocks in fully-integrated CMOS image-rejection, direct conversion, or low-IF receiver and transmitter systems [1]. They are also used to form high-frequency push-push VCO [2]. The design procedure of QVCO is as follows: (1) finding the LC-resonator often based on right-handed (RH) transmission line (TL) structures or scarcely with left-handed (LH) structures [3, 4], (2) combining the LC-resonator with active transistors to form the differential VCOs in cross-coupled, Colpitts, or Clapp form, and (3) using two differential VCOs and passive or active coupling devices or a composite to ensure the two VCOs run in quadrature phase. The most popular QVCOs [5, 6] with parallel-coupled or bottom/top-series coupling transistors can be analyzed with the method described in [5], and the coupling

devices may introduce the injection flicker noise and degrade the phase noise of oscillator. When large coupling MOSFETs are used the power consumption increases. The passive coupling devices include inductor [7], transformer [8], capacitor, diode [9], varactor, and resistor. The passive devices may provide the phase shift of 90° in the QVCO outputs and introduce less injection current noise to the LC-resonator.

The basic unit cell of the RH TL comprises a series inductor L_R and a shunt capacitor C_R as shown in Figure 1(a). The unit cell of the left-handed (LH) TL shown in Figure 1(b) consists of a series capacitor C_L and shunt inductor L_L. There are various composite right/left-handed (CRLH) TL structures can be formed with inductors and capacitors, two CRLH TLs are shown in Figures 1(c) and 1(d). The RH TL has been used to design the differential VCO [10] and the LH TL has been used to design the differential VCO [3] and QVCO [4] with cross-coupled switching transistors; however the performance of 2-stage LH LC-ring oscillator requires further improvement using active coupling between two LC stages for quadrature generation.

This letter proposes new high-performance CMOS QVCO consisted of two differential Colpitts cross-coupled VCOs [11] coupled via four pairs of varactors to provide the quadrature phase. The varactor coupling in the proposed QVCO provides the uni-directivity to the output signal phases which can not be obtained using the MIM capacitor coupling. And the diode coupling [9] penalizes the phase noise because of forward-conduction diode. The finalized QVCO uses the composite TL resonator shown in Figure 1(d) and the Colpitts negative resistance cell. The implemented QVCO was fabricated in the $0.18\,\mu$m CMOS technology and is operated in the X-band. The figure of merit (FOM) of this QVCO is $-189.7\,$dBc/Hz.
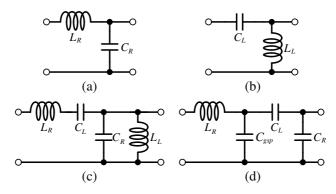

Figure 1. Units of LC resonator. (a) Equivalent-circuit model of a unit cell of the RH TL. (b) Equivalent-circuit model of a unit cell of the LH TL. (c) Composite LH/RH TL. (d) Proposed composite TL.
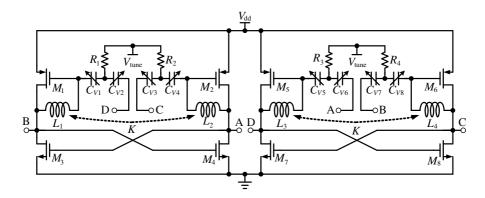
Figure 2. Schematic of the proposed Colpitts QVCO using the composite TL resonator.

2. CIRCUIT DESIGN

Figure 2 shows the proposed QVCO circuit with two differential Colpitts oscillators combined into one QVCO. The pMOSFET M_1, inductor L_1 form a single-ended Colpitts oscillator with the current source M_3. The pMOSFET M_2, inductor L_2 form the second single-ended Colpitts oscillator with the current source M_4. A differential oscillator is obtained by coupling the previous two p-core Colpitts oscillators with the cross-coupled nMOS transistors M_3 and M_4. A second differential oscillator is formed with the inductors L_3 and L_4, pMOSFETs M_5 and M_6, and nMOS transistors M_7 and M_8. The QVCO is formed with the previous two differential oscillators and the coupling accumulation-mode MOS varactors ($C_{v1} \sim C_{v8}$). The varactor capacitance is a function of tuning voltage V_{tune} used for frequency tuning. The resistors $R_1 \sim R_4$ are used for varactor biasing, have large resistance, and contribute small current noise to the VCO. It is well known that a transformer-based LC tank VCO has a high quality factor [12] and L_1 and L_2 (L_3 and L_4) are configured as a transformer to improve the phase noise. Four nMOSFET common-source amplifiers with the gate wired to the drain of pMOSFET are used for measurement purposes.

Figure 3 shows a simplified small-signal equivalent circuit of the proposed QVCO, which uses the composite TL shown in Figure 1(d) in Mobius-connection. The inductor L_R represents $L_1 \sim L_4$ without the mutual coupling effect for simplicity. C_L is the capacitance of varactor C_{v1} in series with C_{v2}. C_R is the capacitance of C_{dsp} in shunt with C_{gsn} and C_{dsn}. The C_{dsp} (C_{dsn}) and C_{gsp} (C_{gsn}) are
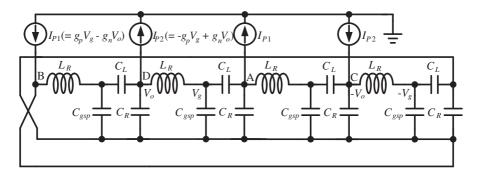
Figure 3. Simplified small-signal equivalent circuit of the proposed QVCO.

respectively the drain-source capacitance and gate-source capacitance of the pMOSFET (nMOSFET). The current source I_{p1} $(= g_p V_g - g_n V_o)$ is the drain current due to the pMOSFET M_1 (M_2) and the drain current due to the nMOSFET M_3 (M_4). I_{p2} $(= -g_p V_g + g_n V_o)$ is the drain current due to the pMOSFET M_5 (M_6) and the drain current due to the nMOSFET M_7 (M_8). The component g_p represents the transconductance of transistors (M_1, M_2, M_5, M_6) and the component g_n is the transconductance of transistors (M_3, M_4, M_7, M_8). V_g and V_o are respectively the gate voltage and drain voltage of M_5. The current sources represent the cross-coupled nMOSFET switching transistors and p-core Colpitts negative cell to supply energy to replenish the energy loss due to the parasitic inductor and varactor resistors, which are not shown in Figure 3 for simplicity. From Figure 3, the ideal oscillation frequency of QVCO is given by

$$\omega_o = \sqrt{\frac{C_{gsp} + 2C_L + C_R}{L_R(C_{gsp}C_L + C_L C_R + C_{gsp}C_R)}} \tag{1}$$

where $C_L = C_v/2$, $C_R = C_{gsn} + C_{dsn} + C_{dsp}$. C_v is the capacitance of $C_{v1} \sim C_{v4}$. The oscillation frequency is function of inductance, capacitance of varactor and active capacitance, and the tuning range is determined by the amount of fixed capacitance versus available capacitance in the circuit. L_R in (1) is replaced by $(L_R + M)$ when the mutual inductance M is considered. The phase shift across a set of components (C_L, C_R, C_{gsp}, L_R) is 90° so that the phase shift of the coupling varactor-inductor loop is 360° and the waveforms of gate voltages (and drain voltages) of pMOSFETs are quadrature. The low-frequency flicker current noises associated with I_{p1} and I_{p2} are respectively injected to the node A (B) and C (D) to modulate the

capacitance of varactor C_L and the oscillation frequency leading to the AM-PM up-converted phase noise. If the C_L in Figure 3 is replaced by a MIM capacitor, the circuit is a quadrature oscillator without phase directivity and tuning function because MIM is a bias-independent uni-polar device. The capacitance of MIM capacitor depends on the absolute voltage value across the capacitor and is independent of bias polarity. If the C_L in Figure 3 is replaced by a single varactor or diode, the circuit is also a quadrature oscillator with phase directivity because the capacitance of varactor or diode is dependent on the bias-direction and bias-magnitude. The diode is forward-biased when the anode voltage is higher than the cathode voltage, and it is equivalent to a diffusion capacitor in shunt with a resistor to degrade the Q-factor of resonator. The capacitance of A-mode MOS varactor depends both on the absolute voltage value across the capacitor and polarity of bias, the capacitance of varactor C_{v1} with anode voltage (gate voltage) > cathode voltage (source voltage) is larger that of the anode voltage < the cathode voltage. In the former case, the MOS varactor operates in the accumulation region, while the latter operates in the depletion region. To include the frequency tuning capability into the quadrature oscillator, many approaches can be used. One way is to replace the C_L with a MIM capacitor in series with a varactor, the tuning voltage is applied to the common node of the MIM capacitor and the varactor. In the proposed quadrature VCO, a pair of back-to-back varactors is used for C_L, the instantaneous capacitance of varactor varies during one period of oscillation. Because of bias-polarity dependence, the series connection of C_{v1} and C_{v2} is relatively insensitive to instantaneous bias variation as compared with the MIM-varactor pair with the same
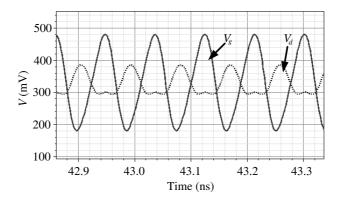

Figure 4. Simulated voltage waveforms of V_g (solid line) and V_d (dotted line). $V_{\mathrm{dd}} = 1.2\,\mathrm{V}$ and $V_{\mathrm{tune}} = 0\,\mathrm{V}$.

dc capacitance. This reduces the phase noise due to the AM-PM upconversion [13]. If the voltage swings at the two terminals of a pair of back-to-back varactors are the same, the varactor pair can not be used to set the phase directivity. Simulation result in Figure 4 shows that the gate voltage swing V_g of pMOSFET M_1 is higher than the drain voltage V_d of M_1. The drain voltage swing is respectively limited by the ground and supply voltage levels through the nMOSFET and pMOSFET, however the gate voltage can swing above the supply voltage and below the ground level. Since the effective capacitance of varactor depends not only on control voltage, but also on the amplitude of oscillation, the gate voltage swing higher than the drain voltage provides the unidirectivity of output quadrature phase (B, A, D, C) because the net current will flow from a high-voltage terminal of the varactor pair to the low-voltage terminal. This can not be predicted by the ac small-signal model shown in Figure 3 as the oscillator output is a large signal. Simulation shows that the QVCO provide quadrature phase outputs across the whole tuning range.

3. MEASUREMENT RESULTS

The QVCO was designed and fabricated in the TSMC 0.18 μm 1P6M CMOS technology. Figure 5 shows the micrograph of the QVCO with a chip area of $0.478 \times 0.82\,\text{mm}^2$ including the pads. Two 4-port 4-turn octagonal transformers are used as the resonator inductors. The circuit simulation was carried out by the simulation tool Specter-RF. The simulated tool ADS Momentum was used to simulate the parameters of transformers. On board measurements of output spectra and output power were obtained using the Agilent E4407B spectrum analyzer. The power consumption of QVCO core is 20.4 mW at the supply voltage of 1.5 V.
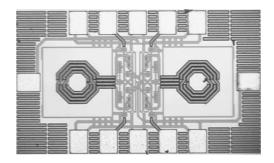

Figure 5. Chip photograph of the proposed QVCO.

The oscillating frequency can be tuned from 9.69 GHz to 10.52 GHz as shown in Figure 6 while the tuning voltage V_{tune} varies from 0 V to 2 V. As V_{tune} increases, the capacitance of varactor decreases and the oscillation frequency increases. Figure 6 shows that the output-frequency-tuning voltage relation can be approximately described by $\omega_o = \omega_o(0) + k_v V_{\text{tune}}$ with the VCO gain $k_v = 0.45$ GHz/V. Linear $k_v \, (= \partial\omega_o/V_{\text{tune}})$ improves the settling behavior of phase-locked loops. An optimal varactor plays two roles for VCO frequency tuning and for coupling the two differential VCOs. If the size of varactor is large, k_v is large leading to large phase noise and tuning range
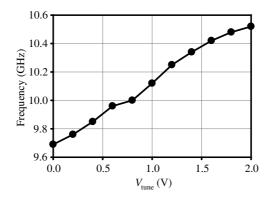
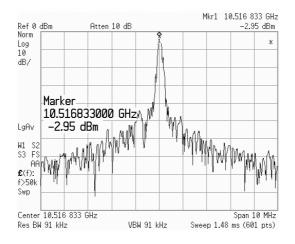**Figure 6.** Measured tuning range of the QVCO. $V_{\text{dd}} = 1.5$ V.

Figure 7. Measured spectrum of the QVCO at 10.52 GHz. $V_{\text{dd}} = 1.5$ V, $V_{\text{tune}} = 2$ V.

and efficient coupling. If the size of varactor is small, tuning range is small and phase error increases. Figure 7 shows the measured frequency spectrum at 10.52 GHz of the QVCO, and the output power is -2.95 dBm. Figure 8 shows the measured phase noise at the oscillation frequency of 10.52 GHz. The phase noise is -122.41 dBc/Hz
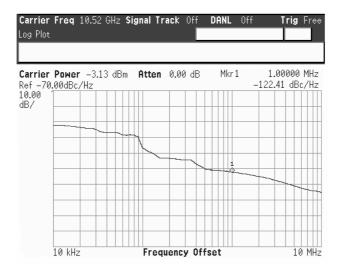

Figure 8. Measured phase noise of the proposed quadrature VCO. $V_{dd} = 1.5$ V, and fosc $= 10.52$ GHz.
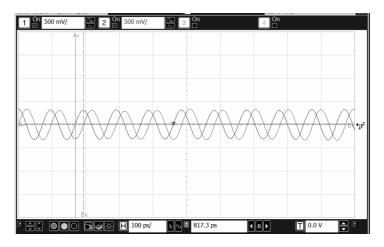

Figure 9. Measured output waveforms of the I and Q channels. $V_{dd} = 1.5$ V and fosc $= 10.27$ GHz.

at 1 MHz offset frequency. Figure 9 shows the measured time-domain output waveforms of two QVCO output buffers by using the Agilent 54855A Infiniium oscilloscope. The output phase error is 0.15°. Measured data shows the IQ operation similar to the simulation result with the phase error between 0.15° and 1.2°.

The figure of merit (FOM) is a useful performance measured used to evaluate the performance of a QVCO relative to its alternative QVCOs. It combines many important design parameters and may include the operating frequency, phase noise, purity of the output waveform, power consumption, tuning range, output power, chip size, phase error and technology. A QVCO designer can use the FOM as an excellent benchmarking tool. In the QVCO, the pMOSFETs and nMOSFETs in the signal path exhibit cyclostationary noise behavior, requiring the use of periodically varying noise statistics in analysis because the ac bias conditions are periodic functions of time. The figure of merit (FOM) [14] of this proposed QVCO is -189.7 dBc/Hz,

Table 1. Comparison of CMOS VCO Performance.

Ref.	VCO Topology	Tech. (μm)	Freq. (GHz)	V_{DD} (V)/ P_{DC} (mW)	PN (dBc/Hz)
[3]	Cross-coupled	0.09	21	-/14	-100.8
[3]	Cross-coupled	0.09	55	-/14	-86.7
[4]	Cross-coupled	0.13	5.12	0.506/4.05	-126.1
[16]	Clapp	0.18	7.89	0.9/12.2	-118.65
[17]	Cross-coupled	0.18	10.3	1.8/-	-117.5
[18]	Cross-coupled	0.18	9.15	1.8/9	-118.67
This	Colpitts-cross-coupled	0.18	10.52	1.5/20.4	-122.41

Ref.	FOM (dBc/Hz)	Coupling method	Phase error	Phase outputs	-
[3]	-175.8	-	-	2	-
[3]	-170	-	-	2	-
[4]	-194.2	MIM cap	-	8	-
[16]	-185.71	MOSFET	-	4	-
[17]	-187.5	MOSFET	-	4	-
[18]	-177.3	MOSFET	0.5°	4	-
This	-189.7	Varactor	0.15°	4	-

and it is defined as

$$\text{FOM} = L\{\Delta\omega\} + 10 \cdot \log\left(\frac{P_{\text{DC}}}{1\,\text{mW}}\right) - 20 \cdot \log\left(\frac{\omega_o}{\Delta\omega}\right) \qquad (2)$$

where ω_o is the oscillating frequency, P_{DC} is the DC power consumption of the measured QVCO. The phase noise is a crucial important parameter, in Equation (2) the phase noise $L\{\Delta\omega\}$ decreases as the power consumption increases to enhance the strength of carrier power. Increasing the signal power improves the signal/noise ratio simply because the thermal noise is fixed. According to the theory of the impulse sensitivity function (ISF) [15], the current noise charges the tank's capacitor, and the developed voltage across the capacitor modulates the phase of oscillator and the phase noise is proportional to the last term $20\log(\Delta\omega/\omega_o)$. The modulation is a mixing process leading to the AM-PM conversion. The phase noise due to the AM-PM in varactors is a function of the VCO gain k_v, a constant k_v indicates that the phase noise is slightly independent of V_{tune}. VCO output amplitude variations due to the low-frequency noise injection can also modulate the phase delay associated with the nMOSFETs and pMOSFETs. The signal swing of the QVCO causes the operating point of the MOSFETs to vary periodically and the MOSFETs exhibit an AM-PM transfer function that is dependent on its operating characteristics. Table 1 lists the comparison of VCO performance. The FOM performance is better than the QVCO in [19].

4. CONCLUSION

A prototype Colpitts cross-coupled QVCO has been proposed and successfully implemented in the TSMC $0.18\,\mu\text{m}$ 1P6M CMOS technology; and it is designed to operate in the $10.0\,\text{GHz}$ frequency band and has the figure of merit of $-189.7\,\text{dBc/Hz}$. The QVCO is tunable from $9.69\,\text{GHz}$ to $10.52\,\text{GHz}$. The high-performance QVCO uses two p-core Colpitts n-cross coupled oscillators and a ring LC resonator to form the QVCO circuit. The coupling varactors are used to control the phase directivity of QVCO, the tuning range, and the phase shift of outputs. The proposed QVCO has the advantage of active-coupling QVCO to set the output phase directivity and without the drawback of active coupling QVCO to inject coupling device noise. Besides the parasitic capacitance of active coupling transistors is absent in the proposed QVCO, this leads to potential high-frequency and wide-tuning range application. And the QVCO uses the back-to-back varactor configuration to reduce the AM-PM upconversion and noise and unbalanced voltage swings to drive the varactor-pair and set the

output phase directivity. The experimental results prove the QVCO circuit using the composite TL structure is useful for RF circuit design.

ACKNOWLEDGMENT

REFERENCES

1. Lee, S. Y. and C. Y. Chen, "Analysis and design of a wide-tuning-range VCO with quadrature outputs," *IEEE Trans. Circuits and Systems II: Express Briefs*, Vol. 55, No. 12, 1209–1213, Dec. 2008.

2. Yazdi, A. and M. M. Green, "A 40 GHz differential push-push VCO in 0.18 μm CMOS for serial communication," *IEEE Microw. Wireless Compon. Lett.*, Vol. 19, No. 11, 725–727, Nov. 2009.

3. Yu, A. H.-T., S.-W. Tam, Y. Kim, E. Socher, W. Hant, M.-C. F. Chang, and T. Itoh, "A dual-band millimeter-Wave CMOS oscillator with left-handed resonator," *IEEE Trans. Microw. Techni.*, Vol. 58, No. 5, 1401–1409, May 2010.

4. Li, G. and E. Afshari, "A low-phase-noise multi-phase oscillator based on left-handed LC-ring," *IEEE J. Solid-State Circuits*, Vol. 45, No. 9, 1822–1833, Sep. 2010.

5. Rofougaran, A., J. Rael, M. Rofougaran, and A. Abidi, "A 900 MHz CMOS LC-oscillator with quadrature outputs," *IEEE ISSCC Dig. Tech. Papers*, 392–393, Feb. 1996.

6. Andreani, P. and X. Wang, "On the phase-noise and phase-error performances of multiphase LC CMOS VCOs," *IEEE J. Solid-State Circuits*, Vol. 39, No. 11, 1883–1893, Nov. 2004.

7. Jang, S.-L., C.-C. Shih, C.-C. Liu, and M.-H. Juang, "A 0.18 μm CMOS quadrature VCO using the quadruple push-push technique," *IEEE Microw. Wireless Compon. Lett.*, Vol. 20, 343–345, Jun. 2010.

8. Chuang, Y.-H., S.-H. Lee, R.-H. Yen, S.-L. Jang, and M.-H. Juang, "A low-voltage quadrature CMOS VCO based on voltage-voltage feedback topology," *IEEE Microw. Wireless Compon. Lett.*, Vol. 16, No. 12, 696–698, Dec. 2006.

9. Jang, S.-L., C.-W. Chang, H.-A. Yeh, M.-H. Juang, and Y.-J. Song, "CMOS quadrature VCOs using the diode coupling technique," *Micro. and Opti. Tech. Lett.*, Vol. 53, No. 3, 551–553, Mar. 2011.

10. Jang, S.-L., C.-Y. Chiu, and C.-F. Lee, "A complementary Colpitts VCO implemented with ring inductor," *IEEE Int. VLSI-DAT*, 23–25, Apr. 2008.

11. Jang, S.-L., C.-F. Lee, and C.-W. Chang, "A K-band differential Colpitts cross-coupled VCO in 0.13 μm CMOS," *Solid-State Electron.*, Vol. 53, No. 9, 931–934, Sep. 2009.

12. Baek, D., T. Song, E. Yoon, and S. Hong, "8-GHz CMOS quadrature VCO using transformer-based LC tank," *IEEE Microw. Wireless Compon. Lett.*, Vol. 13, No. 10, 446–448, Oct. 2003.

13. Wei, M. D., S. F. Chang, and Y. J. Yang, "A CMOS backgate-coupled QVCO based on back-to-back series varactor configuration for minimal AM-to-PM noise conversion," *IEEE Microw. Wireless Compon. Lett.*, Vol. 19, No. 5, 320–322, May 2009.

14. Ham, D. and A. Hajimiri, "Concepts and methods in optimization of integrated LC VCOs," *IEEE J. Solid-State Circuits*, Vol. 36, No. 6, 896–909, Jun. 2001.

15. Lee, T. H. and A. Hajimiri, "Oscillator phase noise: A tutorial," *IEEE J. Solid-State Circuits*, Vol. 35, No. 3, 326–336, Mar. 2000.

16. Jang, S.-L., H.-A. Yeh, C.-W. Chang, M.-H. Juang, and H.-S. Chen, "A quadrature CMOS Clapp voltage-controlled oscillator," *Microw. Opt. Technol. Lett.*, Vol. 53, No. 8, 1909–1911, Aug. 2011.

17. Ko, S., T. Song, E. Yoon, and S. Hong, "A transformer-based X-band CMOS quadrature without current sources," *Microw. Opt. Technol. Lett.*, Vol. 44, No. 4, 305–307, Feb. 2005.

18. Chamas, I. R. and S. Raman, "An X-band superharmonic injectioncoupled quadrature VCO (IC-QVCO) with a tunable tail filter for I/Q phase calibration," *IEEE RFIC Symp.*, 123–126, 2007.

19. Shie, C.-I., J.-C. Cheng, S.-C. Chou, and Y.-C. Chiang, "Design of CMOS quadrature VCO using on-chip trans-directional couplers," *Progress In Electromagnetics Research*, Vol. 106, 91–106, 2010.